

# Characterization of the rat Na<sup>+</sup>/nucleoside cotransporter 2 and transport of nucleoside-derived drugs using electrophysiological methods

Ignacio M. Larráyo, Alonso Fernández-Nistal, Aitziber Garcés, Edurne Gorraitz, and M. Pilar Lostao

Department of Physiology and Nutrition, University of Navarra, Pamplona, Spain

Submitted 11 March 2006; accepted in final form 10 July 2006

**Larráyo, Ignacio M., Alonso Fernández-Nistal, Aitziber Garcés, Edurne Gorraitz, and M. Pilar Lostao.** Characterization of the rat Na<sup>+</sup>/nucleoside cotransporter 2 and transport of nucleoside-derived drugs using electrophysiological methods. *Am J Physiol Cell Physiol* 291: C1395–C1404, 2006. First published July 12, 2006; doi:10.1152/ajpcell.00110.2006.—The Na<sup>+</sup>-dependent nucleoside transporter 2 (CNT2) mediates active transport of purine nucleosides and uridine as well as therapeutic nucleoside analogs. We used the two-electrode voltage-clamp technique to investigate rat CNT2 (rCNT2) transport mechanism and study the interaction of nucleoside-derived drugs with the transporter expressed in *Xenopus laevis* oocytes. The kinetic parameters for sodium, natural nucleosides, and nucleoside derivatives were obtained as a function of membrane potential. For natural substrates, apparent affinity ( $K_{0.5}$ ) was in the low micromolar range (12–34) and was voltage independent for hyperpolarizing membrane potentials, whereas maximal current ( $I_{max}$ ) was voltage dependent. Uridine and 2'-deoxyuridine analogs modified at the 5-position were substrates of rCNT2. Lack of the 2'-hydroxyl group decreased affinity but increased  $I_{max}$ . Increase in the size and decrease in the electronegativity of the residue at the 5-position affected the interaction with the transporter by decreasing both affinity and  $I_{max}$ . Fludarabine and formycin B were also transported with higher  $I_{max}$  than uridine and moderate affinity ( $102 \pm 10$  and  $66 \pm 6$   $\mu$ M, respectively). Analysis of the pre-steady-state currents revealed a half-maximal activation voltage of about –39 mV and a valence of about –0.8.  $K_{0.5}$  for Na<sup>+</sup> was 2.3 mM at –50 mV and decreased at hyperpolarizing membrane potentials. The Hill coefficient was 1 at all voltages. Direct measurements of radiolabeled nucleoside fluxes with the charge associated showed a ratio of two positive inward charges per nucleoside, suggesting a stoichiometry of two Na<sup>+</sup> per nucleoside. This discrepancy in the number of Na<sup>+</sup> molecules that bind rCNT2 may indicate a low degree of cooperativity between the Na<sup>+</sup> binding sites.

two-electrode voltage clamp; concentrative nucleoside transport; pre-steady-state currents

NUCLEOSIDE TRANSPORTERS are integral membrane proteins responsible for the uptake into the cells of natural nucleosides and nucleoside-derived drugs used in anticancer and antiviral therapies (5, 9, 12). In mammalian cells, these transporters belong to two main transporter families: the equilibrative nucleoside transporter (ENT) family, with broad substrate selectivity, and the Na<sup>+</sup>-dependent concentrative nucleoside transporter (CNT) family (3, 9, 12). Three isoforms of the CNT family have been cloned so far. They differ in their substrate selectivity: CNT1 (N2 system) is pyrimidine preferring, CNT2 (N1 system) is purine preferring and also transports uridine, and CNT3 (N3 system) shows broad selectivity, accepting both

pyrimidine and purine nucleosides (9, 10, 12). CNT1 and CNT2 are located in the apical membrane of specialized epithelial cells in small intestine, kidney, and liver and are also expressed in brain, spleen, pancreas, and skeletal muscle. They are responsible for the transepithelial flux of the nucleosides and nucleoside drugs in combination with the ENT transporters located at the basolateral membrane (3, 12).

Function of human CNT1 (hCNT1) and hCNT3 has been extensively studied using electrophysiological techniques (15, 29, 30), and the substrate selectivity has been investigated for these two isoforms as well as for human CNT2 in different expression systems (8, 13–15, 21, 23, 27–30, 36). Previous studies of substrate selectivity of rat CNT2 (rCNT2) have been performed through inhibitory experiments (4, 16, 17) and with electrophysiological methods at a fixed membrane potential and substrate concentration (8). Nevertheless, a complete electrophysiological characterization of rCNT2 has not been performed yet. Therefore, the goal of the present work has been to characterize rCNT2 function and obtain structural information of its substrates by using the two-electrode voltage-clamp technique applied to *Xenopus laevis* oocytes expressing the transporter. We have directly determined the Na<sup>+</sup>-nucleoside stoichiometry and obtained the kinetic parameters ( $K_{0.5}$  and  $I_{max}$ ) for sodium, natural nucleosides, and relevant nucleoside-derived drugs as a function of membrane potential. We also have shown that rCNT2 exhibits pre-steady-state and Na<sup>+</sup>-leak currents. The structural requirements of rCNT2 substrates are compared with those for hCNT2, suggesting that the rat could be a good model for the studies of bioavailability of possible drugs substrates of CNT2.

## MATERIALS AND METHODS

**Nucleosides.** All nucleoside derivatives used in this study are anticancer drugs, with the exception of formycin B, which is used in the treatment of intestinal parasites, and 5-ethyl-2'-deoxyuridine (Et-dUrd), which has antiviral properties; 5-iodouridine (IUrd) and 2'-deoxyuridine (2'dUrd) have been tested only in cell lines. Gemcitabine was purchased from the University Hospital (University of Navarra, Pamplona, Spain). The rest of the nucleosides and derivatives were obtained from Sigma (Alcobendas, Madrid, Spain).

**Expression of rCNT2 in *Xenopus laevis* oocytes.** Stage VI oocytes from *Xenopus laevis* (Blades Biological, Cowden, UK) were obtained as previously described (1). They were microinjected with 50 ng of mRNA coding for the rCNT2 cloned from rat blood-brain barrier (16). Rat CNT2 clone was kindly donated by Drs. W. M. Pardridge and R. J. Boado (University of California, Los Angeles, CA). Oocytes were maintained at 18°C in Barth's medium [88 mM NaCl, 1 mM KCl, 0.33 mM Ca(NO<sub>3</sub>)<sub>2</sub>, 0.41 mM CaCl<sub>2</sub>, 0.82 mM MgSO<sub>4</sub>, 2.4 mM

Address for reprint requests and other correspondence: M. P. Lostao, Departamento de Fisiología y Nutrición, Universidad de Navarra, c/Irunlarrea 1, Pamplona 31080, Spain (e-mail: plosta@unav.es).

The costs of publication of this article were defrayed in part by the payment of page charges. The article must therefore be hereby marked "advertisement" in accordance with 18 U.S.C. Section 1734 solely to indicate this fact.

NaHCO<sub>3</sub>, and 10 mM HEPES-Tris, pH 7.4] containing gentamycin (50 mg/l). Experiments were performed at 22 ± 1°C, 2–4 days after injection.

**Electrophysiology.** The electrophysiology experiments were performed using the two-microelectrode voltage-clamp method (1, 19, 24). The oocyte membrane potential was normally held at a potential of −50 mV, and continuous current data were recorded using Axoscope V1.1.1.14 (Axon Instruments, Foster City, CA). To obtain the current/voltage relationship, we applied 11 pulses of potential (test potential) between +50 and −150 mV (−20 mV decrement) for 100 ms using pCLAMP 6 software (Axon Instruments). The jump from the holding potential to the test potential generates the “on” current, and the return from the test potential to the holding potential, before the next jump, generates the “off” current.

**Steady-state kinetics.** The apparent affinity constant ( $K_{0.5}^S$ ) and the maximal current ( $I_{\max}^S$ ) for saturating nucleoside concentrations were obtained by fitting the steady-state currents ( $I$ ) at each membrane potential to the following equation:

$$I = I_{\max}^S \cdot [S]^n / [(K_{0.5}^S)^n + [S]^n] \quad (1)$$

where  $[S]$  is the nucleoside concentration (7 concentrations from 2 μM to 1 mM or from 50 μM to 10 mM, depending on the nucleoside) and  $n$  is the Hill coefficient, which was 1 for nucleoside kinetic analysis. The fit was performed using the nonlinear fitting method in SigmaPlot 8 (SPSS, Chicago, IL).

For Na<sup>+</sup> activation experiments, saturating concentrations of uridine (0.5 mM) were applied as NaCl concentration was varied between 0 and 100 mM (0.1, 0.3, 0.5, 1, 2, 5, 20, and 100 mM), substituting choline for Na<sup>+</sup>. Uridine-dependent currents, at each voltage, were fitted to Eq. 1, where, in this case,  $I$  is the uridine-induced steady-state current,  $I_{\max}^S$  is the maximal uridine current at saturating Na<sup>+</sup> concentrations,  $[S]$  is the Na<sup>+</sup> concentration,  $K_{0.5}^S$  is the sodium concentration at half-maximal current, and  $n$  is the Hill coefficient.

**Charge-to-nucleoside stoichiometry.** To determine Na<sup>+</sup>-to-nucleoside coupling stoichiometry, we directly compared unidirectional [<sup>3</sup>H]adenosine uptake into voltage-clamped oocytes with the cotransporter (substrate-induced) currents over the same time course in individual oocytes (6, 15, 18). The nonspecific uptakes of [<sup>3</sup>H]adenosine in noninjected oocytes were <1% of the rCNT2-specific uptakes.

The oocyte was voltage-clamped at −50 mV and superfused with 100 mM Na<sup>+</sup> medium. When the baseline was stable, 0.1 mM [<sup>3</sup>H]adenosine was added to the Na<sup>+</sup> solution at a final concentration of 1.4 nCi/μl. After 5–10 min, the nucleoside was removed from the bathing solution, and the oocyte was superfused with Na<sup>+</sup> buffer until the current returned to the baseline. The oocyte was recovered from the chamber, rinsed three times in ice-cold choline buffer, and solubilized with 10% SDS for liquid scintillation counting. Uptake was expressed as picomoles per oocyte. [<sup>3</sup>H]adenosine uptake in noninjected oocytes was used to correct for endogenous adenosine uptake. Adenosine-induced current was obtained as the difference between baseline current and the current obtained after addition of adenosine and was integrated to obtain total adenosine-dependent charge ( $Q_{\text{adenosine/adenosine}}$ ). This charge was converted to its molar equivalent using the Faraday's constant.

**Pre-steady-state currents.** The pre-steady-state transient currents observed after voltage steps are attributed to changes in the conformation of the transporter (11, 19). These capacitive currents were separated from the membrane capacitance and the steady-state conductances using the fitted method (11). The transporter-mediated charge at each membrane potential was then calculated by integrating the transporter-transient currents with time. In most cases, the “off” transient was analyzed. The charge-voltage ( $Q/V$ ) relationships obtained were fitted to the Boltzmann equation

$$(Q - Q_{\text{hyp}})/Q_{\text{max}} = 1/[1 + \exp\{z(V_t - V_{0.5})F/RT\}] \quad (2)$$

where  $Q_{\text{max}} = Q_{\text{dep}} - Q_{\text{hyp}}$ ,  $Q_{\text{dep}}$  and  $Q_{\text{hyp}}$  are the charges moved at depolarizing and hyperpolarizing limits, respectively,  $z$  is the apparent valence of the movable charge,  $V_t$  is the test potential,  $V_{0.5}$  is the voltage at which the charge was equally distributed between depolarizing and hyperpolarizing limits,  $F$  is Faraday's constant,  $R$  is the gas constant, and  $T$  is the absolute temperature. The charge/voltage relationship was obtained in the presence of different Na<sup>+</sup> concentrations (0.5, 1, 2, 5, 20, and 100 mM) and  $Q_{\text{max}}$  was calculated for each concentration.

## RESULTS

**Kinetic parameters for natural nucleosides and derivatives.** We initially studied the substrate selectivity of rCNT2 in oocytes clamped at −50 mV. As shown in Fig. 1, 1 mM adenosine or uridine, natural substrates of the N1 transport system, induced Na<sup>+</sup> inward current, indicating that they are substrates of rCNT2. Similarly, 1 mM of the two purine-derived drugs fludarabine and formycin B and the uridine derivative 5-fluoro-5'-deoxyuridine (5'-Dfur) also induced inward current, demonstrating that they are transported. Unexpectedly, the cytidine derivative gemcitabine, substrate of the N2 transport system (21), evoked inward current at 1 mM, although it was very small. The higher currents induced by the drugs compared with adenosine or uridine currents at saturating concentration (see  $K_{0.5}$  values in Fig. 3) suggest a higher transport rate for the nucleoside derivatives. As happens in other Na<sup>+</sup>-dependent transporters, in the absence of substrate and the presence of Na<sup>+</sup>, rCNT2 shows a baseline current that is not present when the oocyte is perfused with Na<sup>+</sup>-free buffer (Fig. 1D) or in noninjected oocytes (Fig. 1E); this current is referred to as the Na<sup>+</sup>-leak current through rCNT2.

We then studied the influence of the membrane potential on the kinetic parameters of the natural substrates of rCNT2 and the nucleoside-derived drugs. Figure 2A shows the  $I_{\max}/V$  relationship for uridine and inosine, another natural purine nucleoside.  $I_{\max}$  was voltage-dependent for both nucleosides, increasing at hyperpolarizing membrane potentials, although  $I_{\max}$  for inosine was lower than that for uridine at all membrane potentials (~40% at −50 mV).  $K_{0.5}$  was voltage independent at hyperpolarizing membrane potentials for the two nucleosides and was also lower for inosine: at −50 mV,  $K_{0.5}$  was 8.0 ± 0.3 and 20 ± 3 μM for inosine and uridine, respectively (Fig. 2B). Figure 3 summarizes the  $K_{0.5}$  values and maximal currents expressed as percentages of uridine current at saturating concentration for the natural nucleosides at −50 mV of membrane potential. Considering the errors, apparent affinity and  $I_{\max}$  were similar for adenosine, guanosine, and uridine, whereas inosine showed a slight increase in affinity and an ~50% reduction in  $I_{\max}$ . Thymidine and cytidine, substrates of CNT1, can be also transported by rCNT2, although with lower affinity and  $I_{\max}$  (Fig. 3).

$I_{\max}$  was also voltage dependent for fludarabine (Fig. 2C), 5'-Dfur, and formycin B (data not shown) and was higher than  $I_{\max}$  for uridine at all membrane potentials. Figure 2D shows the  $K_{0.5}/V$  relationship for fludarabine, 5'-Dfur, and uridine.  $K_{0.5}$  was voltage independent at hyperpolarizing membrane potentials for the three nucleosides, being higher for fludarabine and 5'-Dfur (4-fold and 1 order of magnitude, respectively) than for uridine (see Fig. 4).  $K_{0.5}$  for formycin B was

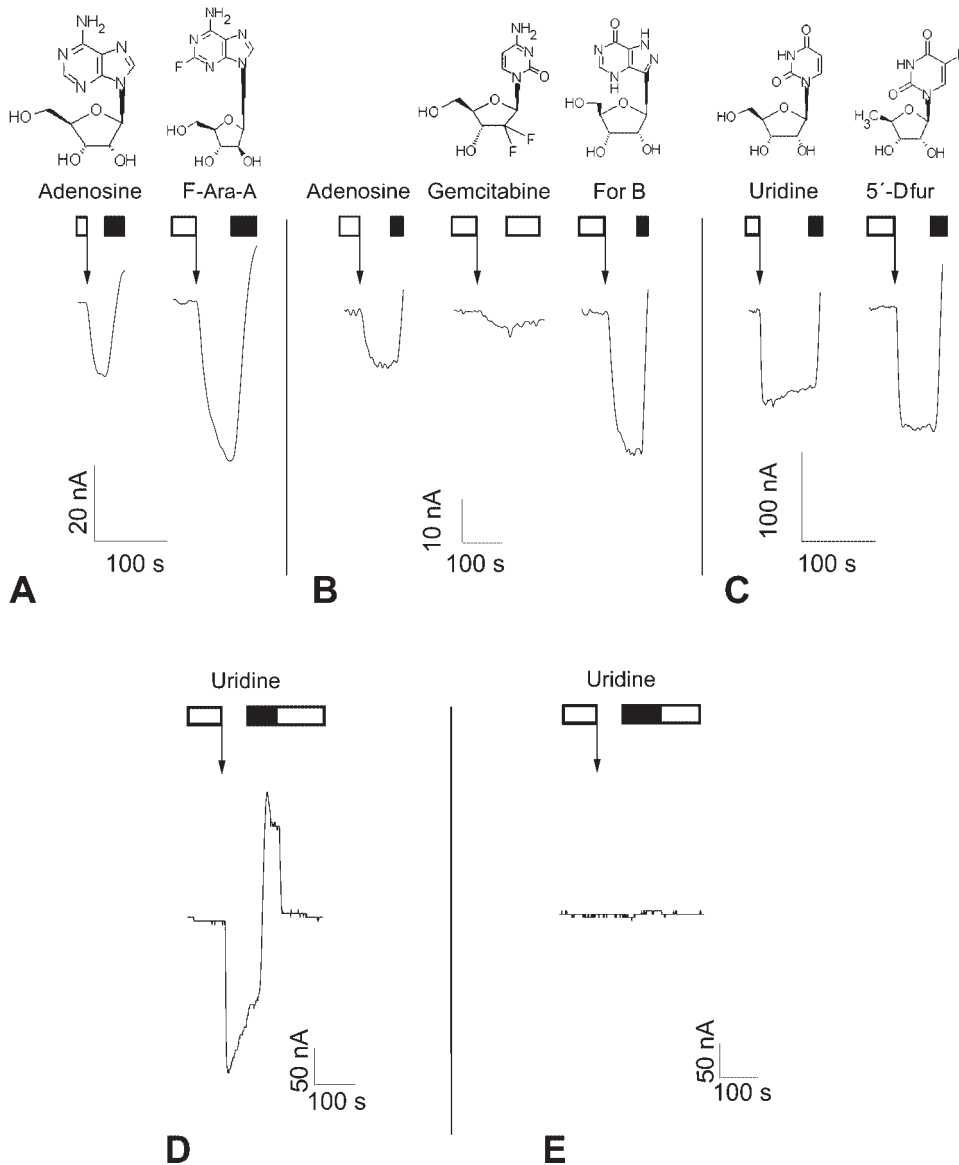


Fig. 1. Interaction of nucleoside-derived drugs with the rat  $\text{Na}^+$ -dependent concentrative nucleoside transporter CNT2 (rCNT2). A–C: rCNT2-expressing oocytes were held at  $-50$  mV of membrane potential and perfused with  $\text{Na}^+$  buffer in the absence of substrate (open box), and current was continuously recorded (baseline current). A: addition of 1 mM adenosine (arrow) induced an inward current of 20 nA. The oocyte was then washed out with  $\text{Na}^+$ -free buffer (filled box), which blocked the adenosine inward current and the baseline current. After the perfusion with  $\text{Na}^+$  buffer, the current returned to baseline. The addition of 1 mM fludarabine (F-Ara-A) induced an inward current 2-fold higher than adenosine current, indicating that it is transported. B: in a different oocyte the current induced by 1 mM formycin B (For B) was also double the current induced by 1 mM adenosine. Gemcitabine (1 mM) induced a very small current. C: 1 mM 5-fluoro-5'-deoxyuridine (5'-Dfur) induced higher inward current than 0.5 mM uridine. D: a rCNT2-expressing oocyte was held at  $-50$  mV of membrane potential and perfused with  $\text{Na}^+$  buffer in the absence of substrate (open box), and current was continuously recorded (baseline current). The addition of 0.5 mM uridine induced an inward current of  $\sim 200$  nA. This current and the baseline current disappeared when the oocyte was washed out with  $\text{Na}^+$ -free buffer (filled box). The oocyte was then perfused with  $\text{Na}^+$  buffer, and the baseline current was restored; this current is referred to as the  $\text{Na}^+$ -leak current. E: in a noninjected oocyte from the same batch as the oocyte in D, no uridine-induced current or  $\text{Na}^+$ -leak current was obtained.

two to three times higher than for uridine (see Fig. 4). Another six uridine derivatives with anticancer or antiviral activities were tested and their kinetic parameters obtained as a function of membrane potential. Figure 4 summarizes the  $K_{0.5}$  values and maximal currents expressed as percentages of uridine current at saturating concentration, at  $-50$  mV of membrane potential, for all tested derivatives.

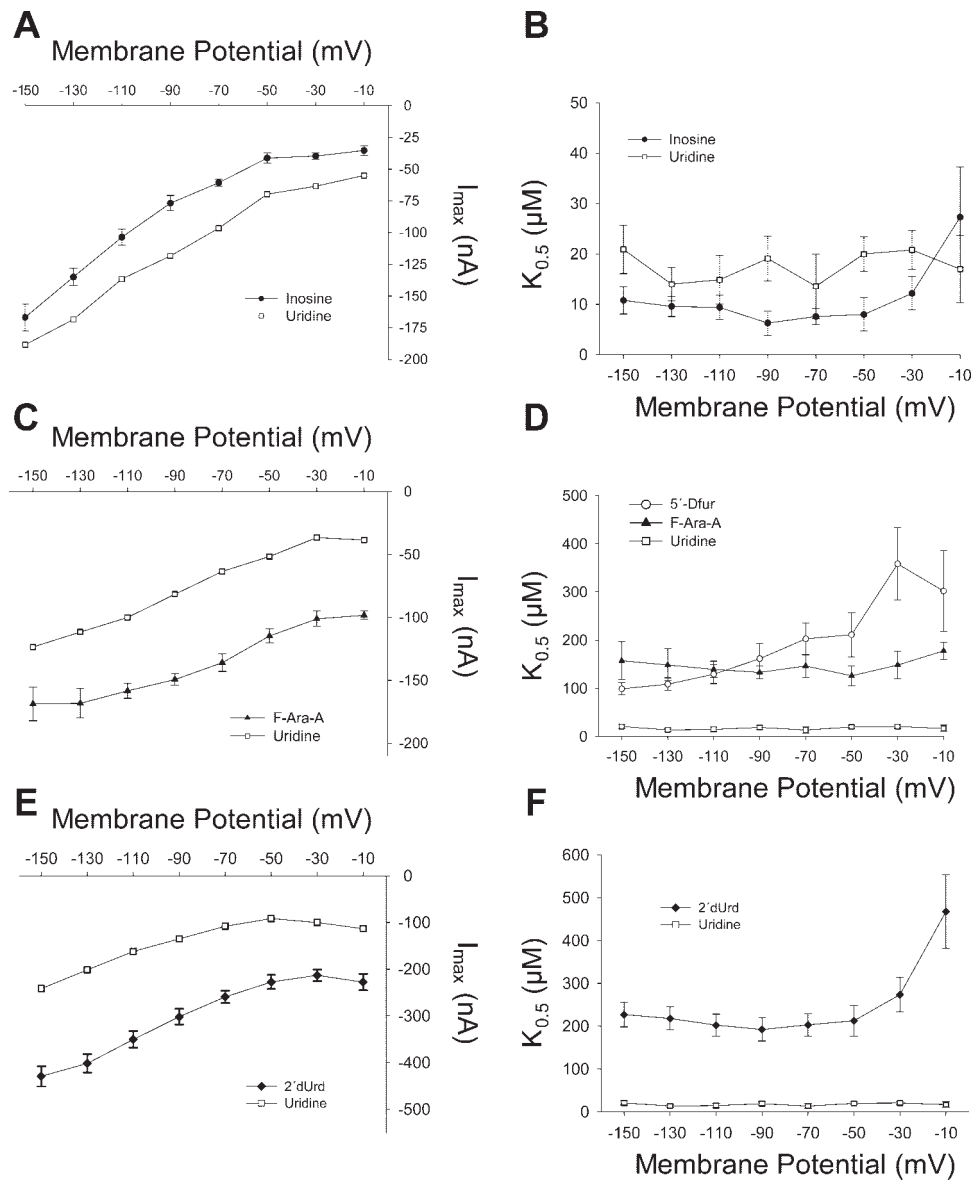
Kinetic parameters for 5-fluorouridine (FUrd) are similar to those for uridine (Fig. 4). However, IUrd showed much lower affinity ( $\sim 18$ -fold) and an  $\sim 30\%$  decrease in  $I_{\max}$ . In the case of 2'-dUrd, there was an increase in  $K_{0.5}$  ( $\sim 6$ -fold) and  $I_{\max}$  ( $\sim 2.5$ -fold) (Fig. 2, E and F, and Fig. 4). Similarly, 5-fluoro-2'-deoxyuridine (FdUrd) showed increase in both kinetic parameters ( $\sim 7$ -fold for  $K_{0.5}$  and  $\sim 20\%$  for  $I_{\max}$ ). In 5-bromo-2'-deoxyuridine (BrdUrd), the presence of the bromine in the 5-position of the pyrimidine ring further decreased affinity ( $\sim 1$  order of magnitude) and also diminished  $I_{\max}$  ( $\sim 60\%$ ) (Fig. 4). In thymidine, or 5-methyl-2'-deoxyuridine, the methyl group in the 5-position also decreased affinity and  $I_{\max}$  in the same

degree as did the bromine atom (Fig. 3). When an ethyl group is in the same position (EtdUrd), there is a further increase in the affinity ( $1,127 \pm 287 \mu\text{M}$ ) and a decrease in  $I_{\max}$  ( $\sim 80\%$ ) compared with uridine kinetic parameters. Table 1 shows the ratio  $I_{\max}/K_{0.5}$ , a measure of the transport efficiency, for all the nucleosides and derivatives.

Since  $I_{\max}$  for 2'-dUrd, 5'-Dfur, and fludarabine was higher than for uridine, these nucleoside derivatives were also tested, at 1 mM concentration, in noninjected oocytes to check that they did not induce any unspecific current. None of them induced current in the control oocytes, indicating that the higher currents evoked by those nucleosides in rCNT2-expressing oocytes were therefore solely due to the transporter.

**$\text{Na}^+$  activation kinetics.** The rCNT2-mediated uridine-evoked currents were measured as a function of  $\text{Na}^+$  concentration at  $-10$ ,  $-30$ ,  $-50$ ,  $-70$ , and  $-90$  mV (Fig. 5). These dose-response activation curves were fitted to Eq. 1 to obtain the kinetic parameters for  $\text{Na}^+$  and the Hill coefficient.  $K_{0.5}^{\text{Na}^+}$  decreased at hyperpolarizing membrane potentials from 6.5

Fig. 2. Voltage dependence of apparent affinity ( $K_{0.5}$ ) and maximal current ( $I_{max}$ ) for uridine, inosine, fludarabine (F-Ara-A), 5'-Dfur, and 2-deoxyuridine (2'dUrd). For each nucleoside,  $K_{0.5}$  and  $I_{max}$  were obtained at every membrane potential by fitting the steady-state currents obtained at 7 different concentrations (2–5,000  $\mu$ M) to Eq. 1 in MATERIALS AND METHODS. A, C, and E: current-voltage ( $I_{max}$ -V) curves for uridine and inosine (A), fludarabine (C), or 2'dUrd (E) were obtained in 3 different oocytes. The uridine curve corresponds to the inward current at saturating uridine concentration (0.5 mM), which is equivalent to the  $I_{max}$ . B, D, and F:  $K_{0.5}$ -V curves for inosine (B), fludarabine and 5'-Dfur (D), and 2'dUrd (F) were obtained. Uridine  $K_{0.5}$  is also shown for comparison. The error bars correspond to the error of the fit. Similar results were obtained with oocytes from at least 3 different batches.



mM at  $-10$  mV to  $0.25$  mM at  $-90$  mV (Fig. 5F). The Hill coefficient was 1 for all membrane potentials (Fig. 5G). To determine whether rCNT2 can be driven by  $H^+$ , as has been shown for hCNT3 (30), we measured uridine-induced current in choline buffer (absence of  $Na^+$ ) at pH 6. No current was observed, indicating that protons do not interact with rCNT2 (data not shown). Experiments performed to resolve whether  $K^+$  or  $Cl^-$  are involved in the nucleoside transport by rCNT2 and contribute to generate the current revealed that none of them altered the nucleoside-induced current (data not shown). These results, therefore, indicate that the current evoked by the nucleoside transport is due only to the cotransport of  $Na^+$ . **rCNT2 stoichiometry.** To determine charge/nucleoside stoichiometry, we measured nucleoside-induced current and [ $^3H$ ]adenosine uptake in the same rCNT2-expressing oocyte over an equal time course. Figure 6, inset, shows an example of an oocyte clamped at  $-50$  mV and superfused with  $100$  mM  $Na^+$  buffer, which produced the baseline current due to the

$Na^+$  leak through the transporter. The addition of  $0.1$  mM [ $^3H$ ]adenosine induced an inward current of  $\sim 18$  nA during 9 min of perfusion. When the nucleoside was removed from the bath, the current returned to the baseline. The current was integrated with time to determine the adenosine-dependent net charge influx ( $Q^{adenosine}$ ) that was  $9.9 \times 10^{-6}$  C (coulomb) of positive charge. This charge was converted to its molar equivalent,  $103$  pmol, and compared with the [ $^3H$ ]adenosine uptake,  $62$  pmol, resulting in a charge-to-nucleoside ratio of  $1.7$  for this oocyte. The same process was repeated with six oocytes. All the data were fitted to a single regression line. For all oocytes tested, the value of  $Q^{adenosine}/adenosine$  uptake was  $1.9 \pm 0.2$  (Fig. 6), indicating that two net inward positive charges were transported for every nucleoside cotransported, which is a different result of coupling stoichiometry from that obtained using the Hill coefficient (Fig. 5; see DISCUSSION). **Pre-steady-state currents.** Similar to other cotransporters, in the presence of  $Na^+$  and absence of substrate, rCNT2 shows pre-steady-state currents that disappear upon addition of uri-



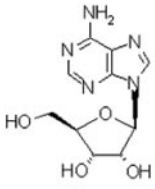
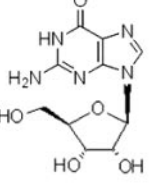
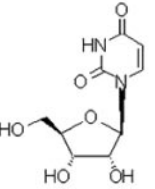
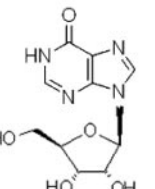
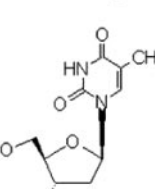
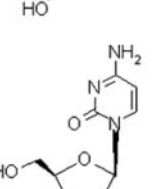
		$K_{0.5}$ ( $\mu$ M)	% 0.5 mM Uridine current
	<b>Adenosine</b>	<b>18<math>\pm</math>4</b>	<b>82<math>\pm</math>10 (7)</b>
	<b>Guanosine</b>	<b>34<math>\pm</math>3</b>	<b>123<math>\pm</math>20 (10)</b>
	<b>Uridine</b>	<b>24<math>\pm</math>6</b>	<b>100 (7)</b>
	<b>Inosine</b>	<b>12<math>\pm</math>4</b>	<b>53<math>\pm</math>8 (6)</b>
	<b>Thymidine</b>	<b>423<math>\pm</math>93</b>	<b>40<math>\pm</math>11 (4)</b>
	<b>Cytidine</b>	<b>505<math>\pm</math>128</b>	<b>29<math>\pm</math>4 (4)</b>

Fig. 3. Structure, apparent affinity constant, and maximal current for natural nucleosides.  $K_{0.5}$  values were calculated, at  $-50$  mV membrane potential, by fitting the currents generated by the substrate at 7 concentrations ( $2 \mu$ M– $10$  mM) to *Eq. 1* in MATERIALS AND METHODS. Currents induced by saturating nucleoside concentrations ( $I_{\max}$ ) are expressed as percentages of the current generated by saturating uridine concentration ( $0.5$  mM) in the same oocyte. Values are means  $\pm$  SE of 4–10 determinations.

dine (Fig. 7) and are reduced by lowering the external  $\text{Na}^+$  concentration (data not shown). Analysis of these currents revealed a  $V_{0.5}$  of  $-39 \pm 5$  mV ( $n = 22$ ), a  $z$  of  $-0.75 \pm 0.05$  ( $n = 15$ ), and values of  $Q_{\max}$  between 6 and 15 nC, depending on the level of expression of the oocytes. Figure 7, *inset*, shows the charge-voltage relationship of one oocyte expressing rCNT2 for which  $V_{0.5}$  was  $-28 \pm 5$  mV and  $Q_{\max}$  was  $14.4 \pm 0.6$  nC. As happens for other  $\text{Na}^+$ -coupled transporters, in rCNT2 external  $\text{Na}^+$  influenced the  $V_{0.5}$ . There was a shift in  $V_{0.5}$  of  $\sim 20$  mV per  $e$ -fold change in  $\text{Na}^+$  concentration (from 5 to 100 mM). In agreement with the high affinity for  $\text{Na}^+$ ,  $Q_{\max}$  did not change in a wide  $\text{Na}^+$  concentration range (10–100 mM; data not shown).

## DISCUSSION

In the present study we have reported a detailed electrophysiological characterization of the rat purine-preferring nucleoside

side transporter rCNT2 and shown the apparent affinity constant and maximal current of a series of nucleoside-derived drugs, contributing to the knowledge of the structural requirements for nucleoside derivatives transport by rCNT2. The kinetic parameters for natural nucleosides reported presently are in agreement with those obtained using uptake of radiolabeled nucleosides in oocytes or cell lines expressing rCNT2 (16, 32) and similar to those for hCNT2 (13, 28, 33, 36), which has a 81% identity with rCNT2.

Our results indicate that the pyrimidine-nucleosides thymidine and cytidine, typical substrates of CNT1, are transported by rCNT2, although with much lower affinity and maximal current than uridine (Fig. 3). These findings explain why the cytidine-derived drug gemcitabine produces some detectable current (Fig. 1). Other authors (13, 17) have also shown that thymidine is transported by rCNT2 and hCNT2. The kinetic parameters of Furd are similar to those for uridine. The

Fig. 4. Structure, apparent affinity constant, and maximal current for nucleoside-derived drugs transported by rCNT2.  $K_{0.5}$  values were calculated, at  $-50$  mV membrane potential, by fitting the currents generated by the substrate at 7 concentrations ( $2\text{ }\mu\text{M}$ – $10\text{ mM}$ ) to Eq. 1 in MATERIALS AND METHODS.  $I_{\text{max}}$  induced by saturating nucleoside derivative concentrations are expressed as percentages of the current generated by saturating uridine concentration ( $0.5\text{ mM}$ ) in the same oocyte. Values are means  $\pm$  SE of 4–7 determinations.  $K_{0.5}$  value for formycin B corresponds to 1 experiment, and its error is the error of the fit of the experimental data to Eq. 1. FUrd, 5-fluorouridine; IUrd, 5-iodouridine; 2'dUrd, 2'-deoxyuridine; FdUrd, 5-fluoro-2'-deoxyuridine; BrdUrd, 5-bromo-2'-deoxyuridine; EtdUrd, 5-ethyl-2'-deoxyuridine; 5'-Dfur, 5-fluoro-5'-deoxyuridine; F-Ara-A, fludarabine; For B, formycin B.

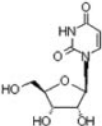
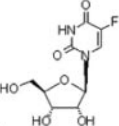
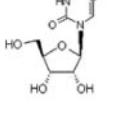
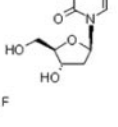
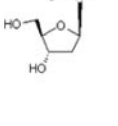
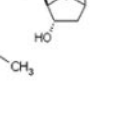
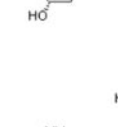
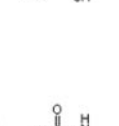

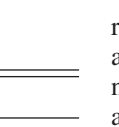
	$K_{0.5}(\mu\text{M})$	% 0.5 mM uridine current
 Uridine	24 $\pm$ 6	100
 FUrd	32 $\pm$ 4	90 $\pm$ 9
 IUrd	443 $\pm$ 44	68 $\pm$ 5
 2'dUrd	157 $\pm$ 35	246 $\pm$ 25
 FdUrd	188 $\pm$ 34	121 $\pm$ 7
 BrdUrd	360 $\pm$ 111	45 $\pm$ 11
 EtdUrd	1127 $\pm$ 287	19 $\pm$ 3
 5'-Dfur	371 $\pm$ 102	137 $\pm$ 41
 F-Ara-A	102 $\pm$ 10	192 $\pm$ 19
 For B	66 $\pm$ 6	215 $\pm$ 13

Table 1. Transport efficiency

Nucleoside	$I_{\text{max}}/K_{0.5}$
Adenosine	4.56 $\pm$ 1.55
Inosine	4.42 $\pm$ 2.13
Uridine	4.17 $\pm$ 1.04
Guanosine	3.62 $\pm$ 0.89
ForB	3.26 $\pm$ 0.49
FUrd	2.81 $\pm$ 0.63
F-A-Ara	1.88 $\pm$ 0.36
2'dUrd	1.57 $\pm$ 0.50
FdUrd	0.64 $\pm$ 0.15
5'-Dfur	0.37 $\pm$ 0.21
IUrd	0.15 $\pm$ 0.03
BrdUrd	0.13 $\pm$ 0.07
Thymidine	0.09 $\pm$ 0.05
Cytidine	0.06 $\pm$ 0.009
EtdUrd	0.02 $\pm$ 0.007

Ratio of maximal current ( $I_{\text{max}}$ ) to apparent affinity ( $K_{0.5}$ ) is a measure of transport efficiency.

replacement of fluorine with iodine (IUrd) decreases apparent affinity and maximal current (Fig. 4). These changes in recognition and transportability may be due to both the bigger size and the smaller electronegativity of the iodine. The same values and changes in kinetic parameters for the two derivatives occur in hCNT2 (13, 14, 36), which indicates that both the rat and human isoforms of CNT2 are equally restrictive to the residue size and electronegativity at the 5-position. Unlike rCNT2, affinity and transport rate for 2'dUrd in hCNT2 are similar to those for uridine (13, 36). In accordance to these results,  $K_i$  and current for 2'-deoxyadenosine are the same as those for adenosine in hCNT2 (13), whereas current for this nucleoside is greater than that for adenosine in rCNT2 (8). All these data indicate that the hydroxyl at this position is more important for the rat than for the human isoform. The chemical structure of FdUrd is a “combination” of the structure of the previous nucleosides. The lack of the hydroxyl

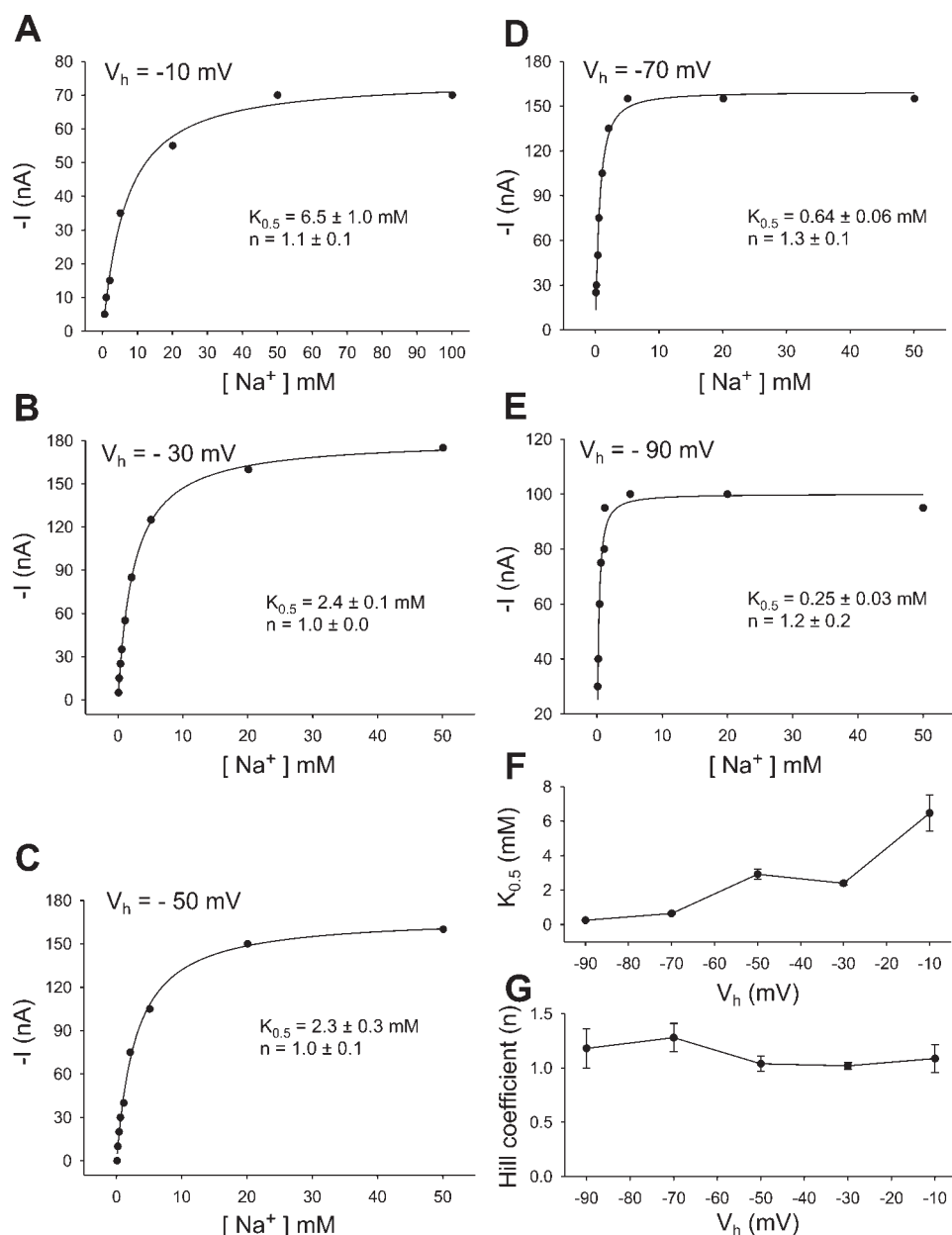


Fig. 5. Na<sup>+</sup> activation curves at different membrane potential ( $V_h$ ). A–E:  $K_{0.5}^{Na^+}$  was obtained by fitting the currents at each Na<sup>+</sup> concentration to Eq. 1 in MATERIALS AND METHODS. Each curve corresponds to a single representative rCNT2-expressing oocyte. Similar results were obtained with oocytes from 3 different batches. F:  $K_{0.5}^{Na^+}$  as a function of  $V_h$ . G: Hill coefficient as a function of  $V_h$ .

residue would increase  $I_{max}$ , as in 2'dUrd, but the fluorine would slightly decrease  $I_{max}$  as for FUr. As a result, there is an increase in maximal current, but not as large as that for 2'dUrd. In hCNT2, affinity and maximal transport rate for FdUrd would be expected to be similar to those for uridine, as shown in one report (13). Recently, however, a  $K_i$  value for FdUrd of  $151 \pm 7 \mu\text{M}$  was reported (36). This  $K_i$  is close to the  $K_{0.5}$  we obtained for rCNT2 ( $188 \pm 34 \mu\text{M}$ ). Strikingly, other authors (8) have not found any detectable current induced by FdUrd in either rCNT2 or hCNT2.

The bigger size and smaller electronegativity of bromine compared with fluorine may explain the decrease in affinity and  $I_{max}$  in BrdUrd (Fig. 4). Likewise, in hCNT2 there is a reduction in these parameters for BrdUrd of magnitude similar to that in rCNT2 (13, 36).

The methyl group in the 5-position of thymidine affects the kinetic parameters in the same degree as BrdUrd (Figs. 3 and

4). Although the methyl group is slightly smaller than the bromine atom, it is a weak electron donor, which suggests that the size of the substituent at the 5-position and its ability for accepting electrons are important for recognition and transport of the nucleoside. This is confirmed by the higher decrease in both affinity and  $I_{max}$  for EtdUrd (Fig. 4). A similar decrease in the affinity for these three uridine derivatives was found for hCNT2 (13, 36).

In 5'-Dfur, since the fluorine does not alter the  $K_{0.5}$  for uridine and slightly decreases  $I_{max}$ , it is the absence of the hydroxyl group in the 5'-position that may explain the modification in the kinetic constants. These results indicate that this position is not a strict requirement for the recognition and transport by rCNT2. However, in hCNT2, 5'-Dfur is transported with much lower affinity and current than uridine (36).

So far, all these data permit us to deduce the following conclusions. The hydroxyl group at the 2'- and 5'-positions are

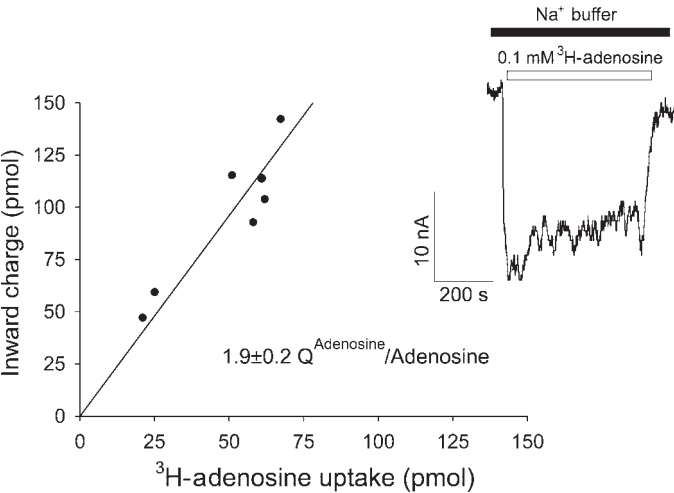


Fig. 6. Charge-to-nucleoside stoichiometry for rCNT2. *Inset*: a representative experiment showing 0.1 mM [<sup>3</sup>H]adenosine-induced inward current in a rCNT2-expressing oocyte. Membrane potential was held at  $-50$  mV, and the oocyte perfused with Na<sup>+</sup> buffer until a stable baseline current was recorded. The addition of 0.1 mM [<sup>3</sup>H]adenosine increased the inward current to  $\sim 18$  nA during 9 min of perfusion. Adenosine was then removed from the bath by perfusing adenosine-free Na<sup>+</sup> buffer, and the current returned to baseline. The transported charge,  $Q$ , was calculated as the integral of the adenosine-dependent current over the 9-min period and was  $9.9 \times 10^{-6}$  C. The [<sup>3</sup>H]adenosine uptake in this oocyte was 62 pmol after subtraction of [<sup>3</sup>H]adenosine uptake, over the same period, in a noninjected oocyte. Uptake of 0.1 mM [<sup>3</sup>H]adenosine in the presence of 100 mM Na<sup>+</sup> and the induced current were measured for 5–10 min in 7 different oocytes as indicated in the *inset*. The adenosine-dependent charge ( $Q^{\text{adenosine}}$ ) for each oocyte was plotted against the uptake of adenosine in the same oocyte. The data were fitted to a linear regression with a slope of  $1.9 \pm 0.2$  charges/adenosine.

not strictly required for transport by rCNT2, because although the lack of either hydroxyl residue decreases the affinity, it enhances the  $I_{\text{max}}$ . On the other hand, increase in the size and decrease in the electronegativity of the residue at the 5-position affect the interaction with the transporter by decreasing the affinity and  $I_{\text{max}}$ . Therefore, a structure with a higher  $I_{\text{max}}/K_{0.5}$  ratio (Table 1) should be that with a substituent at the 5-position of the same size or smaller than fluorine and more electronegative than it. There are no elements that fulfill these requirements, since fluorine is the most electronegative element. Only oxygen, with a slightly bigger size and slightly smaller electronegativity, could be a possible candidate.

The =OH at the 2'-position is more important for binding and transport for rCNT2 than for hCNT2. The =OH at the 5'-position, however, is more important for the human isoform than for the rat one. For both isoforms, the smaller the size of the residue at the 5-position and the higher its ability for accepting electrons, the better the affinity for the transporter.

The only difference between fludarabine (2-fluoro-9-β-D-arabinofuranosyladenine) and adenosine is the presence of a fluorine in the 2-position and that the hydroxyls at 2'- and 3'-positions are in *trans* configuration (Figs. 3 and 4). The affinity of hCNT2 for 9-β-D-arabinofuranosyladenine is approximately threefold lower than for adenosine and even lower for fludarabine (13). On the other hand, it has been demonstrated that 9-β-D-arabinofuranosyladenine is transported by rCNT2 with the same  $I_{\text{max}}$  as adenosine (8). From these data and those in Fig. 4, it could be deduced that the decrease in affinity of rCNT2 for fludarabine may be due to both the *trans*

configuration of the hydroxyl residues at the 2'- and 3'-positions and the fluorine at the 2-position, whereas the increase in  $I_{\text{max}}$  would be due to the presence of fluorine at that position. Formycin B, an inosine derivative, is also transported by murine CNT2 with a  $K_{0.5}$  similar to that reported presently (25, 31).

Except for 2'dUrd and 5'-Dfur, the rest of molecules tested in the present study are equally transported by rat and human CNT2. According to the transport efficiency values in Table 1, with the exception of maybe formycin B, FUrd, and fludarabine, the bioavailability of the derivatives tested is unlikely to be due to transport by CNT2 in the presence of normal levels of the natural nucleosides. The human isoform of CNT1 shows a transport efficiency for FUrd, IUrd, 2'dUrd, FdUrd, and EtdUrd similar to that for uridine (Ref. 29 and unpublished

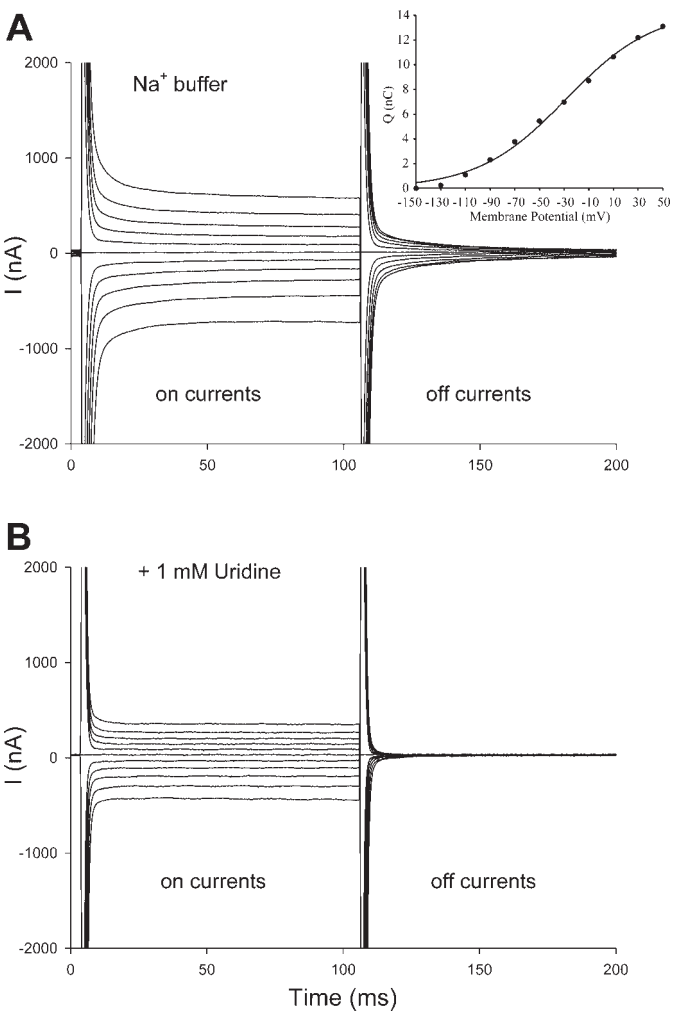


Fig. 7. Membrane current records of rCNT2. *A*: a rCNT2-expressing oocyte was held at  $-50$  mV and stepped to 11 test values between  $+50$  and  $-150$  mV ( $-20$  mV decrement). In Na<sup>+</sup> buffer and in the absence of uridine, the oocyte showed pre-steady-state currents in response to step changes in the membrane voltage and showed steady-state currents due to the Na<sup>+</sup> leak through the transporter. *B*: the addition of 1 mM uridine blocked the pre-steady-state currents and caused an increase of the steady-state inward currents. *Inset*: charge-voltage relationship for a representative oocyte expressing rCNT2. The data (●) were obtained as described in MATERIALS AND METHODS and fitted to the Boltzmann equation (solid line, Eq. 2) from which a  $V_{0.5}$  of  $-28 \pm 5$  was calculated.



data from our laboratory), which suggests that CNT2 may be less relevant than CNT1 in the transport of these drugs. Moreover, hCNT3 also efficiently transports FUr and FdUr and, to a lesser extent, fludarabine (27).

Among the nucleoside derivatives tested, some show decrease and others increase in  $I_{\max}$  compared with uridine or adenosine, similar to hCNT1 (2, 15, 23). Likewise, phenylglucosides induce different maximal currents than the natural sugars when they are transported by the  $\text{Na}^+$ /glucose cotransporter SGLT1 (7, 20). These variations in transportability may be explained by differences in the rate constant for the translocation of the  $\text{Na}^+$ -substrate-loaded cotransporter (7, 20) or the release of the substrate inside the cell. Clearly, the steric constraints, hydrogen bonds, and/or hydrophobic interactions between the nucleoside and the binding site in the transporter determine the affinity and maximal transport rate.

The previously reported apparent affinity constant of rCNT2 for  $\text{Na}^+$ , obtained by measuring adenosine flux in oocytes, was 2.4 mM (16). This value agrees with the present data at  $-30$  mV (Fig. 5B). Therefore, rCNT2 has a high affinity for  $\text{Na}^+$ , close to that reported for hCNT1 (15) and higher than that for human or mouse CNT3 (27).

A  $\text{Na}^+$ :nucleoside stoichiometry of 1:1 has been reported for rCNT2 and the N1 transport system from the analysis of the Hill coefficient (16, 26). On the basis of  $\text{Na}^+$  activation curve analysis, we have also obtained a Hill coefficient of 1. The Hill coefficient is often used as an indirect method to estimate the number of ligand molecules that are required to bind to a transporter to generate transport. However, for a transporter with more than one ligand binding site, "the Hill equation does not reflect a physically possible reaction scheme; only under the very specific condition of marked positive cooperativity (the affinity of the binding has to be very asymmetric, with a much lower affinity of binding for the first ligand molecule than for the subsequent ligand molecules) does the Hill coefficient accurately estimate the number of binding sites. The Hill coefficient is best thought as an 'interaction' coefficient, reflecting the extent of cooperativity among multiple ligand binding sites" (34). Therefore, the Hill coefficient does not always coincides with the stoichiometry obtained using direct methods. We can find an example in SGLT3.  $\text{Na}^+$ -to-sugar stoichiometry for pig SGLT3 (previously called pSGLT2) by direct measurement was found to be 2:1 (6); in the same study the authors reported a Hill coefficient of 1.5, but they quoted a previous study from the same group in which, on the bases of analysis of the  $\text{Na}^+$  Hill coefficient, it was suggested that the pSGLT3 coupling was  $1\text{Na}^+$ :1 sugar (22).

Knowing this limitation of the Hill equation, we wanted in the present work to directly determine the relationship between the inward current and the nucleoside uptake by rCNT2. The results indicate that two inward charges are introduced into the oocyte for each nucleoside that is transported, as occurs in other members of the same family (15, 27, 35). Since  $\text{H}^+$ ,  $\text{K}^+$ , or  $\text{Cl}^-$  are not involved in the uridine-induced inward current, these two charges may be attributable to  $\text{Na}^+$ . The discrepancy between the Hill coefficient and the coupling ratio directly obtained may indicate that the  $\text{Na}^+$  binding in rCNT2 has a low degree of cooperativity between the two  $\text{Na}^+$  binding sites. This stoichiometry would result in an increase in the concentrative capacity of the transporter compared with a stoichiometry of 1:1.

In relation to this result, using direct methods, we previously reported a  $\text{Na}^+$ :nucleoside stoichiometry of 2:1 for hCNT1 (15), different from the 1:1 stoichiometry published by Smith et al. (29). A possible explanation for the differences between their results and ours in the stoichiometry could be related to differences in the methodology.

Rat CNT2 shows pre-steady-state currents in the presence of  $\text{Na}^+$  and absence of substrate that disappear after addition of uridine to the solution and are reduced by lowering the external  $\text{Na}^+$  concentration. As in hCNT1 and other cotransporter families (11, 15, 19, 22, 24, 29), these currents reflect voltage-dependent processes, due to charge movements, caused by  $\text{Na}^+$  binding/dissociation and conformational changes involved in the reorientation of the cotransporter in the membrane. The existence of these currents and their study in depth should be useful in future work to determine inhibitor binding constants and obtain information about the partial reactions of the transport cycle (11, 15, 19), and thereby acquire deeper knowledge of the transport mechanism of the CNT transporter family.

The bioavailability of the drugs, and therefore, the sensitivity or resistance to them, can be the result of the different expression pattern of the nucleoside transporter isoforms in normal and tumoral cells, which is tightly regulated (3, 12). However, without the knowledge of the functional properties of the nucleoside transporters, this issue cannot be properly addressed. The information about the structural requirements of the rCNT2 substrates reported in the present study compared with hCNT2 indicates that in the case of CNT2, the rat could be a good model for the study of particular drugs and supports the relevance of the animal model for the study of drugs bioavailability in vivo.

## ACKNOWLEDGMENTS

We thank A. Redín for technical assistance and Dr. C. Sanmartín for discussion.

## GRANTS

This work has been supported by Plan Investigación Universidad de Navarra, de Navarra Departamento de Educación, and Ministerio de Ciencia y Tecnología (Spanish Government) Grant BFI 2003-01371. I. M. Larráyoz was a recipient of a fellowship from the Asociación de Amigos, Universidad de Navarra.

## REFERENCES

1. Birnir B, Loo DD, and Wright EM. Voltage-clamp studies of the  $\text{Na}^+$ /glucose cotransporter cloned from rabbit small intestine. *Pflügers Arch* 418: 79–85, 1991.
2. Cano-Soldado P, Larráyoz IM, Molina-Arcas M, Casado FJ, Martínez-Picado J, Lostao MP, and Pastor-Anglada M. Interaction of nucleoside inhibitors of HIV-1 reverse transcriptase with the concentrative nucleoside transporter-1 (SLC28A1). *Antivir Ther* 9: 993–1002, 2004.
3. Casado FJ, Lostao MP, Aymerich I, Larráyoz IM, Duflo S, Rodríguez-Mulero S, and Pastor-Anglada M. Nucleoside transporters in absorptive epithelia. *J Physiol Biochem* 58: 207–216, 2002.
4. Che M, Ortiz DF, and Arias IM. Primary structure and functional expression of a cDNA encoding the bile canalicular, purine-specific  $\text{Na}^+$ -nucleoside cotransporter. *J Biol Chem* 270: 13596–13599, 1995.
5. Damaraju VL, Damaraju S, Young JD, Baldwin SA, Mackey J, Sawyer MB, and Cass CE. Nucleoside anticancer drugs: the role of nucleoside transporters in resistance to cancer chemotherapy. *Oncogene* 22: 7524–7536, 2003.
6. Díez-Sampedro A, Eskandari S, Wright EM, and Hirayama BA.  $\text{Na}^+$ -to-sugar stoichiometry of SGLT3. *Am J Physiol Renal Physiol* 280: F278–F282, 2001.

7. Díez-Sampedro A, Lostao MP, Wright EM, and Hirayama BA. Glycoside binding and translocation in Na<sup>+</sup>-dependent glucose cotransporters: comparison of SGLT1 and SGLT3. *J Membr Biol* 176: 111–117, 2000.
8. Gerstin KM, Dresser MJ, and Giacomini KM. Specificity of human and rat orthologs of the concentrative nucleoside transporter, SPNT. *Am J Physiol Renal Physiol* 283: F344–F345, 2002.
9. Gray JH, Owen RP, and Giacomini KM. The concentrative nucleoside transporter family, SLC28. *Pflügers Arch* 447: 728–734, 2004.
10. Griffith DA and Jarvis SM. Nucleoside and nucleobase transport systems of mammalian cells. *Biochim Biophys Acta* 1286: 153–181, 1996.
11. Hazama A, Loo DD, and Wright EM. Presteady-state currents of the rabbit Na<sup>+</sup>/glucose cotransporter (SGLT1). *J Membr Biol* 155: 175–186, 1997.
12. Kong W, Engel K, and Wang J. Mammalian nucleoside transporters. *Curr Drug Metab* 5: 63–84, 2004.
13. Lang TT, Selner M, Young JD, and Cass CE. Acquisition of human concentrative nucleoside transporter 2 (hCNT2) activity by gene transfer confers sensitivity to fluoropyrimidine nucleosides in drug-resistant leukemia cells. *Mol Pharmacol* 60: 1143–1152, 2001.
14. Lang TT, Young JD, and Cass CE. Interactions of nucleoside analogs, caffeine, and nicotine with human concentrative nucleoside transporters 1 and 2 stably produced in a transport-defective human cell line. *Mol Pharmacol* 65: 925–933, 2004.
15. Larráyoiz IM, Casado FJ, Pastor-Anglada M, and Lostao MP. Electrophysiological characterization of the human Na<sup>+</sup>/nucleoside cotransporter 1 (hCNT1) and role of adenosine on hCNT1 function. *J Biol Chem* 279: 8999–9007, 2004. [Corrigenda. *J Biol Chem* 279, October 2004, p. 45290.]
16. Li JY, Boado RJ, and Pardridge WM. Cloned blood-brain barrier adenosine transporter is identical to the rat concentrative Na<sup>+</sup> nucleoside cotransporter CNT2. *J Cereb Blood Flow Metab* 21: 929–936, 2001.
17. Li JY, Boado RJ, and Pardridge WM. Differential kinetics of transport of 2',3'-dideoxyinosine and adenosine via concentrative Na<sup>+</sup> nucleoside transporter CNT2 cloned from rat blood-brain barrier. *J Pharmacol Exp Ther* 299: 735–740, 2001.
18. Loo DD, Eskandari S, Boorer KJ, Sarkar HK, and Wright EM. Role of Cl<sup>−</sup> in electrogenic Na<sup>+</sup>-coupled cotransporters GAT1 and SGLT1. *J Biol Chem* 275: 37414–37422, 2000.
19. Loo DD, Hazama A, Supplisson S, Turk E, and Wright EM. Relaxation kinetics of the Na<sup>+</sup>/glucose cotransporter. *Proc Natl Acad Sci USA* 90: 5767–5771, 1993.
20. Lostao MP, Hirayama BA, Loo DD, and Wright EM. Phenylglucosides and the Na<sup>+</sup>/glucose cotransporter (SGLT1): analysis of interactions. *J Membr Biol* 142: 161–170, 1994.
21. Lostao MP, Mata JF, Larráyoiz IM, Inzillo SM, Casado FJ, and Pastor-Anglada M. Electrogenic uptake of nucleosides and nucleoside-derived drugs by the human nucleoside transporter 1 (hCNT1) expressed in *Xenopus laevis* oocytes. *FEBS Lett* 481: 137–140, 2000.
22. Mackenzie B, Loo DD, Panayotova-Heiermann M, and Wright EM. Biophysical characteristics of the pig kidney Na<sup>+</sup>/glucose cotransporter SGLT2 reveal a common mechanism for SGLT1 and SGLT2. *J Biol Chem* 271: 32678–32683, 1996.
23. Mata JF, García-Manteiga JM, Lostao MP, Fernandez-Veledo S, Guillen-Gomez E, Larráyoiz IM, Lloberas J, Casado FJ, and Pastor-Anglada M. Role of the human concentrative nucleoside transporter (hCNT1) in the cytotoxic action of 5'-deoxy-5-fluorouridine, an active intermediate metabolite of capecitabine, a novel oral anticancer drug. *Mol Pharmacol* 59: 1542–1548, 2001.
24. Parent L, Supplisson S, Loo DD, and Wright EM. Electrogenic properties of the cloned Na<sup>+</sup>/glucose cotransporter: I. Voltage-clamp studies. *J Membr Biol* 125: 49–62, 1992.
25. Patel DH, Crawford CR, Naeve CW, and Belt JA. Cloning, genomic organization and chromosomal localization of the gene encoding the murine sodium-dependent, purine-selective, concentrative nucleoside transporter (CNT2). *Gene* 242: 51–58, 2000.
26. Plagemann PG and Aran JM. Characterization of Na<sup>+</sup>-dependent, active nucleoside transport in rat and mouse peritoneal macrophages, a mouse macrophage cell line and normal rat kidney cells. *Biochim Biophys Acta* 1028: 289–298, 1990.
27. Ritzel MW, Ng AM, Yao SY, Graham K, Loewen SK, Smith KM, Ritzel RG, Mowles DA, Carpenter P, Chen XZ, Karpinski E, Hyde RJ, Baldwin SA, Cass CE, and Young JD. Molecular identification and characterization of novel human and mouse concentrative Na<sup>+</sup>-nucleoside cotransporter proteins (hCNT3 and mCNT3) broadly selective for purine and pyrimidine nucleosides (system cib). *J Biol Chem* 276: 2914–2927, 2001.
28. Ritzel MW, Yao SY, Ng AM, Mackey JR, Cass CE, and Young JD. Molecular cloning, functional expression and chromosomal localization of a cDNA encoding a human Na<sup>+</sup>/nucleoside cotransporter (hCNT2) selective for purine nucleosides and uridine. *Mol Membr Biol* 15: 203–211, 1998.
29. Smith M, Ng AM, Yao SY, Labedz KA, Knaus EE, Wiebe LI, Cass CE, Baldwin SA, Chen XZ, Karpinski E, and Young JD. Electrophysiological characterization of a recombinant human Na<sup>+</sup>-coupled nucleoside transporter (hCNT1) produced in *Xenopus* oocytes. *J Physiol* 558: 807–823, 2004.
30. Smith KM, Slugoski MD, Loewen SK, Ng AM, Yao SY, Chen XZ, Karpinski E, Cass CE, Baldwin SA, and Young JD. The broadly selective human Na<sup>+</sup>/nucleoside cotransporter (hCNT3) exhibits novel cation-coupled nucleoside transport characteristics. *J Biol Chem* 280: 25436–25449, 2005.
31. Vijayalakshmi D and Belt JA. Sodium-dependent nucleoside transport in mouse intestinal epithelial cells. Two transport systems with differing substrate specificities. *J Biol Chem* 263: 19419–19423, 1988.
32. Wang J and Giacomini KM. Molecular determinants of substrate selectivity in Na<sup>+</sup>-dependent nucleoside transporters. *J Biol Chem* 272: 28845–28848, 1997.
33. Wang J, Su S, Dresser MJ, Schaner ME, Washington CB, and Giacomini KM. Na<sup>+</sup>-dependent purine nucleoside transporter from human kidney: cloning and functional characterization. *Am J Physiol Renal Physiol* 273: F1058–F1065, 1997.
34. Weiss JN. The Hill equation revisited: uses and misuses. *FASEB J* 11: 835–841, 1997.
35. Yao SY, Ng AM, Loewen SK, Cass CE, Baldwin SA, and Young JD. An ancient prevertebrate Na<sup>+</sup>-nucleoside cotransporter (hfCNT) from the Pacific hagfish (*Eptatretus stouti*). *Am J Physiol Cell Physiol* 283: C155–C168, 2002.
36. Zhang J, Smith KM, Tackaberry T, Visser F, Robins MJ, Nielsen LP, Nowak I, Karpinski E, Baldwin SA, Young JD, and Cass CE. Uridine binding and transportability determinants of human concentrative nucleoside transporters. *Mol Pharmacol* 68: 830–839, 2005.